East European Journal of Physics. **4.** 289-296 (2024)
DOI:10.26565/2312-4334-2024-4-31 ISSN 2312-4334

INFLUENCE OF BORON DIFFUSION ON PHOTOVOLTAIC PARAMETERS OF n^+-p-p^+ SILICONE STRUCTURES AND BASED PHOTODETECTORS

Mykola S. Kukurudziak[a,b*], Eduard V. Maistruk [b], Ivan P. Koziarskyi [b]
[a]*Rhythm Optoelectronics Shareholding Company, Holovna str. 244, 58032, Chernivtsi, Ukraine*
[b]*Yuriy Fedkovych Chernivtsi National University, Kotsyubyns'kogo str. 2, 58012, Chernivtsi, Ukraine*
**Corresponding Author e-mail: mykola.kukurudzyak@gmail.com*
Received September 1, 2024, revised October 17, 2024 accepted November 15, 2024

The paper investigates the photovoltaic properties of the silicon n^+-p-p^+-structures and photodiodes made on their basis. It was found that boron diffusion to the reverse side of the substrate, in addition to creating an ohmic contact, generates generation-recombination centers, which allows to reduce the dark current of photodiodes and increase their responsivity. It was also found that chemical dynamic polishing of the back side of the substrates before boron diffusion allows to eliminate a significant number of defects and improve the final parameters of the products. In samples without a p^+-layer and samples not polished from the back side, a breakdown of the p-n junction is observed on the back side, which is caused by the expansion of the space charge region to the entire thickness of the substrate and the achievement of a defective back side of the crystal.
Keywords: *Silicon; Photodetectors; Avalanche Photodiode; Dark Curren; Isovalent Impurity; Sensitivity*
PACS: 61.72. Ji, 61.72. Lk, 85.60. Dw

In recent decades, semiconductor photodetectors with one or more p-n junctions have been widely used in optoelectronics, radioelectronics, automation, telemechanics, and other areas of electronics. The interest in photodetectors has especially increased due to the emergence and improvement of various types of coherent and incoherent radiation sources [1, 2]. The development of injection semiconductor LEDs and new types of semiconductor photodetectors based on one or more p-n junctions in miniature and micro-miniature designs has contributed to the rapid development of the field of electronic engineering - optoelectronics, which combines two methods of transmitting and processing information - optical and electrical.

Photodetectors, or photodiodes (PD) with a single p-n junction, are conventional semiconductor diodes with a reverse-biased p-n junction and the ability to irradiate it with a light flux. This class of solid-state electronics devices operates on the basis of the internal photoelectric effect: when radiation is absorbed in the p-n junction or in areas at a distance of the diffusion length of charge carriers from it, nonequilibrium charge carriers are generated, which drift to the p-n junction under the influence of an external electric field, crossing it to increase the photodiode reverse current - the photocurrent [3].

Increased photosensitivity and high-speed performance, as well as a wider spectral and frequency range, are possible with the use of n^+-p-p^+ structures, which form the class of p-i-n PDs. In the p-i-n structure, the i-region is located between two regions of the opposite type of conductivity and has a resistivity 10^6-10^7 times higher than the doped n^+- and p^+-regions. At sufficiently high reverse biases, a strong electric field, the space charge region (SCR), stretches across the entire high-resistance i-region. The photogenerated holes and electrons are quickly separated by the SCR field. In this type of photodetectors, the diffusion of charge carriers (as in p-n photodetectors) is replaced by their drift in the electric field, which creates the basis for a fast, highly sensitive photodetectors [4, 5].

While active n^+-regions are usually formed by the diffusion of impurities of elements of Group V (P, As, Sb, Bi) [6,7], the variability of the formation of an ohmic p^+-layer is much wider: it includes epitaxial growth of a low-resistivity silicon layer [8], grinding or structuring [9], and diffusion of acceptor elements (atoms of Group III - B, Al, Ga, In) [10,11]. Epitaxial growth of the silicon layer, grinding or structuring of the back side of the substrate can cause a decrease in the reflection coefficient from the Au-mirror on the back side, which provides double passage of radiation through the crystal thickness and an increase in the number of photogenerated charge carriers [12]. As for the acceptor impurities, boron diffusion has become widely used [13-15]. Boron diffusion is also used as one of the methods of silicon substrates doping in the process of manufacturing photovoltaic elements [16, 17]. Also, [18] reports on the fabrication of a highly sensitive silicon p^+-n-n^+ PD in the range of λ=200-1000 nm based on black silicon, where the active regions were doped with boron. In [19], silicon PDs for use as low-energy electron detectors have been fabricated using pure-boron technology to form the p^+-anode region. In [20], the technology of a UV avalanche photodiode based on a silicon p^+-in structure with a nanoscale boron doping profile of the responsive regions is described.

It should be noted that the references mainly describe the cases of fabrication and study of detectors with boron-doped photosensitive regions based on n-type Si, and there are very few studies of the effect of boron diffusion to the back side of p-type substrates (as a gettering or ohmic layer) as an isotypic impurity, and, accordingly, the effect of this operation on the parameters of photodetectors has not been studied sufficiently.

Cite as: M.S. Kukurudziak, E.V. Maistruk, I.P. Koziarskyi, East Eur. J. Phys. 4, 289 (2024), https://doi.org/10.26565/2312-4334-2024-4-31

We are also actively studying boron diffusion and its effect on the parameters of *p-i-n* PDs based on *p*-Si. In particular, in [11], we studied the effect of the concentration of doped boron from solid-state planar sources on the efficiency of gettering and the improvement of the dark current and photodiode responsivity. In [11] we investigated the effect of boron concentration on the collection coefficient of nonequilibrium carriers by studying the optical properties of p^+-layers of PDs too. This article describes some of the effects of p^+-layer formation on the photovoltaic properties of n^+-p-p^+-structures and PDs based on them, in particular, the effect of the surface treatment of the back side before diffusion on the final parameters of photodetectors. The study of the photovoltaic properties of these structures is the aim of this work.

EXPERIMENTAL

The research was carried out on the example of silicon four-element *p-i-n* PDs with guard ring (GR) using single-crystal dislocation-free *p*-type FZ-Si with orientation [111], resistivity at $\rho \approx$16-17 kΩ·cm. The structures were prepared using diffusion planar technology in a single process cycle under the same conditions. Three types of structures were produced: n^+-p-structures (PD_{n+-p}) (Fig. 1a), n^+-p-p^+-structures (without polishing the back side of the substrate, $PD'_{n+-p-p+}$), and n^+-p-p^+-structures (with polishing the back side of the substrate, $PD_{n+-p-p+}$) (Fig. 1b). The samples of type PD_{n+-p} were made according to the following technological route: silicon wafers were oxidized; windows in SiO_2 were opened by photolithography for two-stage phosphorus diffusion [7] and formation of n^+-layers (R_S=2.7-2.9 Ω/□), phosphorus-doped layers formed responsive elements (REs) and GR; the masking oxide was etched from the back side of the structures; Cr-Au contacts to the front and back sides were formed by thermal evaporation in vacuum; and to form the final *p-i-n* PDs, the crystals were separated by a diamond disk with an external cutting edge and encased. The $PD'_{n+-p-p+}$ were fabricated according to the same route, but after phosphorus diffusion, boron was diffused to the back side of the substrate from solid-state boron sources according to the methodology described in [11] (R_S=34-40 Ω/□). $PD_{n+-p-p+}$ was manufactured according to the same route as $PD'_{n+-p-p+}$, but before boron diffusion, a chemical dynamic polishing (CDP) operation was performed according to the procedure described in [21] The thickness of the PD_{n+-p} and $PD'_{n+-p-p+}$ crystals was about 510-515 μm, and that of $PD_{n+-p-p+}$ was 495-500 μm. The parameters and photovoltaic properties of the obtained structures were compared.

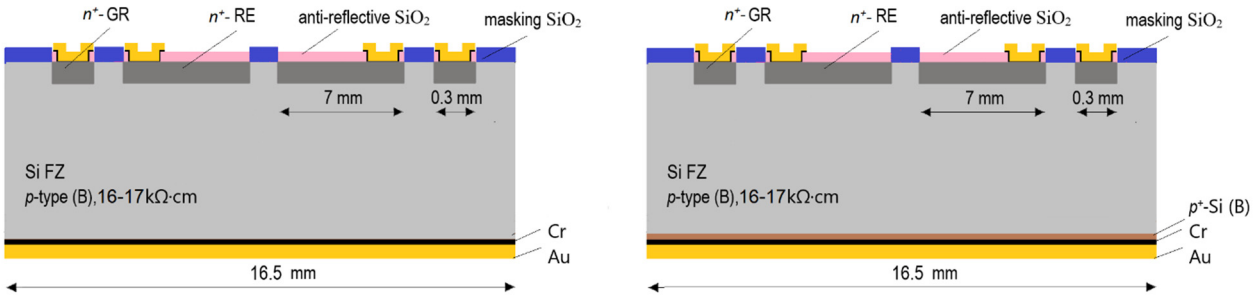

Figure. 1. Schematic cross-section of PD_{n+-p} (a) and $PD'_{n+-p-p+}$ /$PD_{n+-p-p+}$ (b).

The *IV*-characteristics of PDs (dark current (I_d), photocurrent (I_{ph})) were measured using a hardware-software complex implemented on the basis of the Arduino platform, an Agilent 34410A digital multimeter and a Siglent SPD3303X programmable power source, which were controlled by a personal computer using software created by the authors in the LabView environment.

Monitoring of current monochromatic pulse responsivity (S_{pulse}) was carried out by method of comparing responsivity of the investigated PD with a reference photodiode certified by the respective metrological service of the company. Measurements were performed when illuminating the PD with a radiation flux of a power of not over $1 \cdot 10^{-3}$ W; at the reverse bias voltages of $|U_{bias}|$ = 2-270 V and pulse duration τ_i = 500 ns, λ=1064 nm. Measurements of current monochromatic (λ=1064 nm) responsivity on modulated flow (S_{IL}) were performed under illumination of the PD with a modulated radiation flux of f_{mod} = 20 kHz and a power of below $1 \cdot 10^{-3}$ W. Load resistance of the responsive element was R_L = 10 kΩ and operating voltage $|U_{bias}|$ = 1-15 V. The spectral characteristics of photodiode responsivity are also obtained. The measurement was carried out using the KSVU-23 automated spectral complex.

After oxidation and each subsequent thermal operation, the high-frequency volt-farad (*CV*) characteristics of the metal-oxide-semiconductor-structures (MOS) were measured at a frequency of 30 kHz and a probe diameter 1 mm, which made it possible to predict the final parameters of the products.

The capacitance of REs (C_{RE}) was determined at a $|U_{bias}|$=2-120 V.

RESULTS OF THE RESEARCH AND THEIR DISCUSSION

A) Study of the dark currents

When measuring the *IV*-characteristics of the obtained structures, we observed some differences in the values of the I_d: the PD_{n+-p} had the highest dark currents, and the $PD_{n+-p-p+}$ had the lowest (Fig. 2a). The dark current of $PD_{n+-p-p+}$ at $|U_{bias}|$ =140-160 V reached saturation (Fig. 2b), which indicated the expansion of the SCR to the entire thickness of the

crystal, since the volume generation component of the dark current is directly proportional to the width of the SCR [22]. Samples of $PD'_{n+\text{-}p\text{-}p+}$ had a significant spread of dark currents along the RE: in three REs in the range of $|U_{bias}|$=180-200 V, the *p-n* junction breakdown was observed, and the dark current of RE_2 in the range of $|U_{bias}|$=190-200 V reached saturation (Fig. 2c). As for the $PD_{n+\text{-}p}$, their *IV*-characteristics in the range of $|U_{bias}|$=2-230 V acquired a linear character, and at $|U_{bias}|$ = 30-260 V, a breakdown of the *p-n* junction was observed in all REs (Fig. 2d).

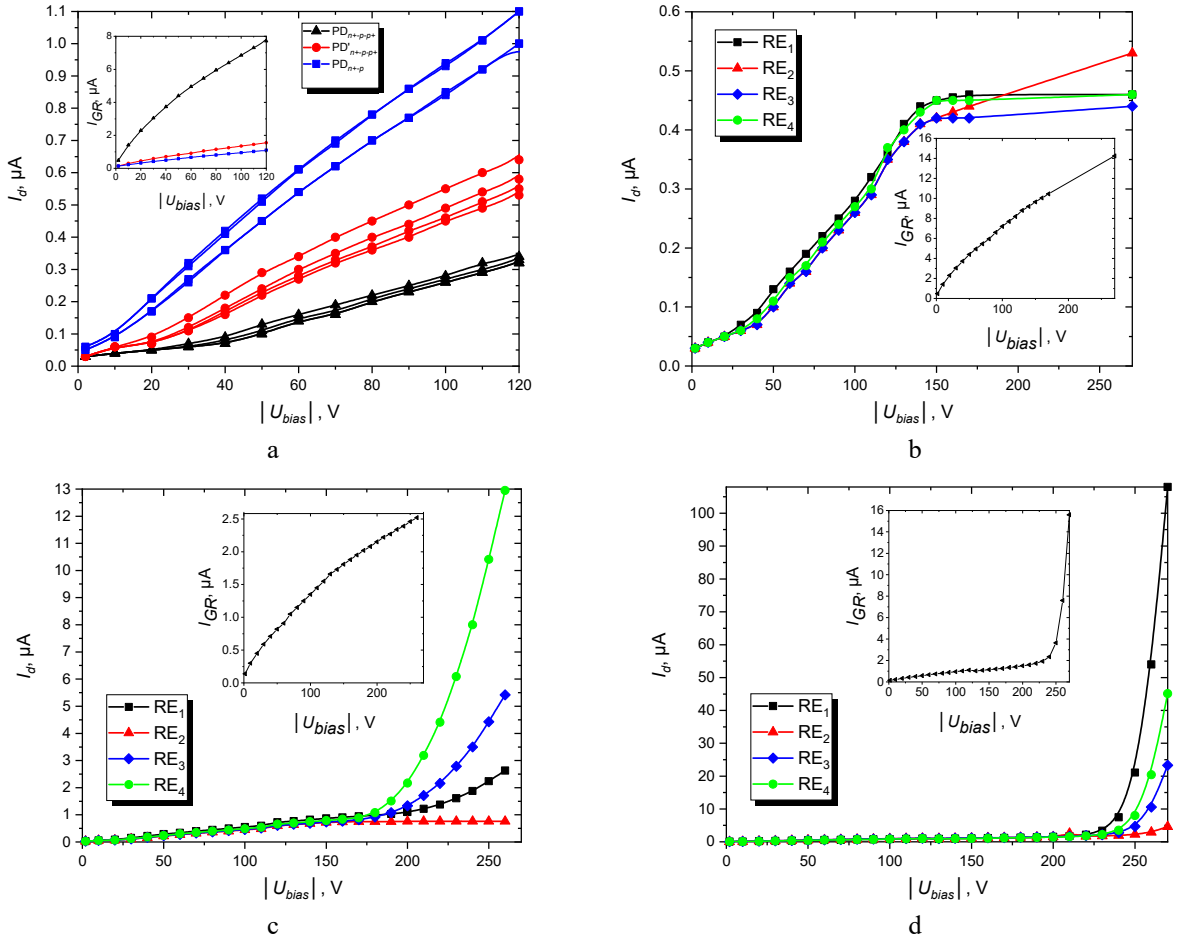

Figure. 2. Reverse dark *I–V*-characteristics of PDs REs and GRs: a) all investigated PDs at $|U_{bias}|$=2-120 V; b) $PD_{n+\text{-}p\text{-}p+}$; c) $PD'_{n+\text{-}p\text{-}p+}$; d) $PD_{n+\text{-}p}$; inserts - *IV*-characteristics of GRs

The difference in the values of the dark currents indicates a different number of generation-recombination centers (GRCs) in the volume of the PD crystals and a different degree of their gettering in the process of manufacturing photodetectors. In the case of $PD_{n+\text{-}p}$, the gettering operations were the predeposition and drive-in of phosphorus into the front side of the PDs, but this gettering process is effective only in the crystal region adjacent to the n^+-layer, and the back side of the and the crystal volume close to it remained saturated with recombination centers, in particular, atoms of uncontrolled impurities and crystallographic defects introduced or created during high-temperature thermal operations. Accordingly, these GRCs make a significant contribution to the level of dark currents of the PDs, and at a high reverse bias voltage (and, accordingly, a high electric field intensity) and when the SCR reaches to the back side of the crystal with defects, the latter provoke an avalanche breakdown [23-25]. It is also known that the breakdown voltage near the surface is lower than in the crystal volume, which also explains the avalanche breakdown when the space charge region of the back side of the crystal is reached [26].

A similar situation applies to the $PD'_{n+\text{-}p\text{-}p+}$, although the backside boron gettering operation is present in the manufacturing route of these PDs, but still, boron gettering is not so effective as to completely eliminate the GRC of the crystal region near the backside of the crystal. Therefore, for the same reasons as in the previous case, breakdown of the *p-n* junction is possible, and a decrease in the breakdown voltage is possible due to the achievement of the SCR of the defective backside of PDs at a lower bias voltage.

It should be noted that this thermal operation of boron diffusion is also an annealing for more efficient gettering by the n^+-layer of the front side of the substrate, which allows diffusion of the deepest uncontrolled impurities to the getter zone. An increase in the annealing time improves the efficiency of GRC elimination. It is worth noting that in [11] we

described a method of effective additional doping of the back side of the substrate by simultaneous diffusion of phosphorus into the front and back sides of the crystal, followed by etching the back n^+-layer before boron diffusion.

The minimum spread and value of I_d were observed in the PD'$_{n+\text{-}p\text{-}p+}$. This was achieved by etching by CDP method the silicon layer of the back side of the substrate saturated with GRC.

It should be noted that the dark currents of the GR (I_{GR}) also had different values and did not reach saturation (Fig. 2 inserts). The I_{GR} depend on the density of surface states and the presence of inversion layers at the interface of Si-SiO_2 at the periphery of the crystal, since with increasing voltage the SCR of GR shift expands not only into the crystal thickness but also towards the periphery.

The samples of PD'$_{n+\text{-}p\text{-}p+}$ and PD$_{n+\text{-}p\text{-}p+}$ had slightly higher values of the I_{GR}, which indicates a higher density of surface states than in PD$_{n+\text{-}p}$. This is also confirmed by the measurement of the insulation resistance between the GR and the REs R_{con}, since this parameter characterizes the presence of conductive inversion channels at the interface of Si-SiO_2 between the active elements: PD$_{n+\text{-}p\text{-}p+}$ -R_{con}=1.4 MΩ, PD'$_{n+\text{-}p\text{-}p+}$ -R_{con}=6.2 MΩ, PD$_{n+\text{-}p}$ -R_{con}=8.7 MΩ. The increase in the conductivity of inversion channels in the case of PD'$_{n+\text{-}p\text{-}p+}$ and PD$_{n+\text{-}p\text{-}p+}$ is caused by the presence of a larger number of thermal operations, unlike PD$_{n+\text{-}p}$, since during the initial thermal operations, atoms of uncontrolled impurities (it can be phosphorus too) diffuse into the surface of silicon oxide, which, during further heat treatments, diffuse to the oxide-silicon interface, and with a significant total duration of heat treatments, can cause a deterioration in the insulation resistance between the active elements and an increase in I_{GR} [27]. The presence of inversion layers can also be assessed by measuring the *CV*-characteristics of MOS structures (Fig. 3), where the curves of PD'$_{n+\text{-}p\text{-}p+}$ and PD$_{n+\text{-}p\text{-}p+}$, which have a longer total duration of thermal operations, can invert.

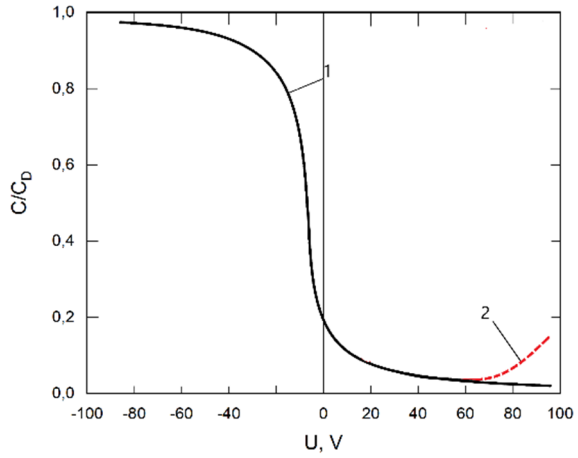

Figure 3. *CV*-characteristics of MOS structures: 1- n^+-*p*-structure
2 – n^+-*n*-p^+--structure

B) Study of the responsivity and photocurrent of PDs

When studying the pulse current monochromatic responsivity, it was seen that the photosensitivity of PD$_{n+\text{-}p\text{-}p+}$ reaches saturation at approximately the same bias voltage as its dark current (Fig. 4, Fig. 5a). This is due to the same reason - the achievement of the maximum width of the SCR, at which further growth of the charge carrier collection coefficient, and, accordingly, responsivity, is impossible (1) [28]. As for the PD'$_{n+\text{-}p\text{-}p+}$, the responsivity of all REs reached saturation around the $|U_{bias}|$ = 180-200 V, as well as the dark current of RE_2, which did not show breakdown. It should be noted that all REs of PD'$_{n+\text{-}p\text{-}p+}$ behaved typically during the responsivity measurement, although some REs showed breakdown at the *IV*-characteristic. The saturation of the samples at different reverse bias voltages indicates the expansion of the SCR to the entire thickness of the crystal at different bias voltages, and, accordingly, the difference in the final resistivity of the *i*-region of the structures (2) [29].

$$S_\lambda = (1-R)TQ\sum\gamma\frac{\lambda_{op}}{1.24} \tag{1}$$

where T is the transmission coefficient of the input window or optical filter; Q is the quantum output of the internal photoeffect, R is the reflection coefficient, γ is the charge carrier collection coefficient.

$$W_i = \left(\frac{2\varepsilon\varepsilon_0(\phi_c - U_{bias})}{eN_A}\right)^{\frac{1}{2}}. \tag{2}$$

where ε, ε_0 are dielectric constants for silicon and vacuum, respectively; φ_c is contact potential difference, N_A is the concentration of acceptors in *i*-region, *e* is the electron charge.

A different picture was observed when measuring the responsivity of n^+-*p*-structures: at a $|U_{bias}|$ = 120 V, a jump-like increase in responsivity was observed (Fig. 4), although according to Fig. 2, the breakdown of the *p*-*n* junction of these

PDs was observed at a voltage of -230-260 V. The S_{pulse} of PD_{n+-p} did not reach saturation, but increased rapidly with increasing bias voltage (Fig. 5b-f) and the responsivity reached the theoretically possible value (3) [28] at $|U_{bias}| \approx$ 230-250 V. Such an increase in responsivity is caused by avalanche breakdown and a significant increase in nonequilibrium charge carriers, similar to an avalanche photodiode. Note that formula (3) is valid for photodetectors without amplifiers or optical concentrators, as well as avalanche photodiodes.

$$S_{\lambda max} = \frac{\lambda}{1.24} \tag{3}$$

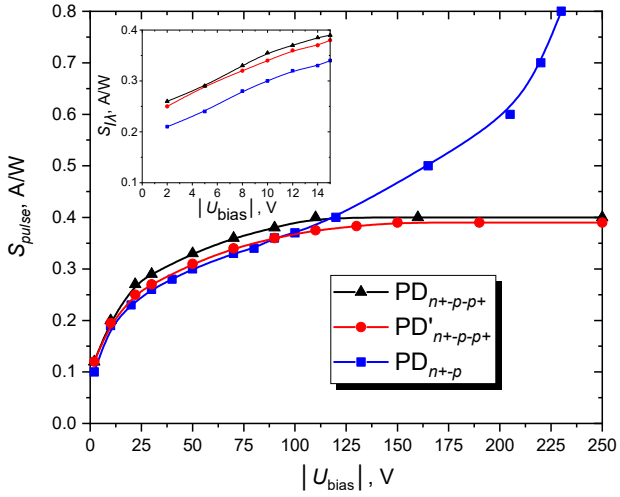

Figure 4. Dependence of the S_{puse} of PDs on the reverse bias voltage (insert $S_{I\lambda}$).

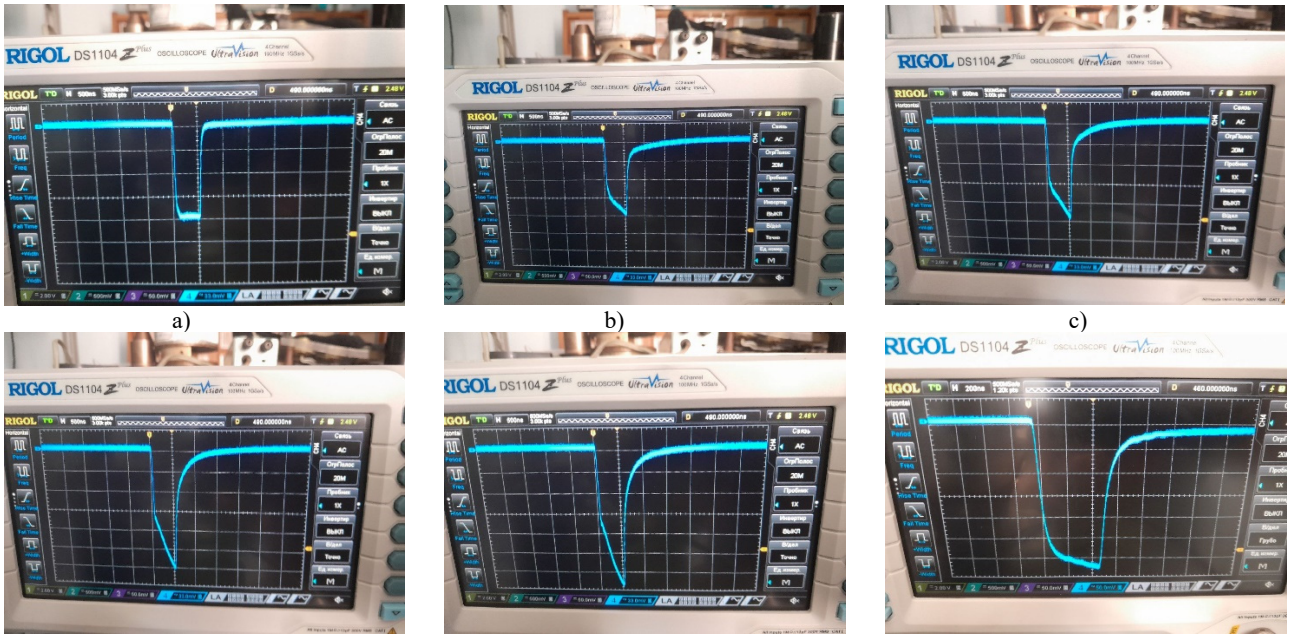

Figure 5. Photodiode pulse waveform: a) $PD_{n+-p-p+}$: $|U_{bias}|$ =160 V, S_{pulse}=0.4 A/W; b) a) PD_{n+-p}: $|U_{bias}|$ =120 V, S_{pulse}=0.4 A/W; c) PD_{n+-p}: $|U_{bias}|$ =165 V, S_{pulse}=0.5 A/W; d) PD_{n+-p}: $|U_{bias}|$ =205 V, S_{pulse}=0.6 A/W; e) PD_{n+-p}: $|U_{bias}|$ =220 V, S_{pulse}=0.7 A/W; f) PD_{n+-p}: $|U_{bias}|$ =240 V, S_{pulse}=0.86 A/W (different scale).

It is worth noting that $PD'_{n+-p-p+}$ and $PD_{n+-p-p+}$ had a slightly higher low-voltage $S_{I\lambda}$ than PD_{n+-p} (Fig. 4 insert). This indicates that $PD'_{n+-p-p+}$ and $PD_{n+-p-p+}$ had a longer diffusion length of minority charge carriers due to more efficient gettering than PD_{n+-p}, and also indicates that at the same voltage, the SCR of PDs with higher responsivity is greater than that of the PD with lower responivity due to lower ρ of *i*-region.

The behavior of light *IV*-characteristics in the visible wavelength range was also studied. It was found that in PD_{n+-p} around a voltage of $|U_{bias}|$ = 120-130 V, a jump-like increase in photocurrent is observed when illuminated with a white light-emitting diode of different illumination (Fig. 6). In the same voltage range, an increase in photocurrent and

sensitivity at a wavelength of 1064 nm is observed. Taking into account the described avalanche-like growth of photocurrent and sensitivity in PD_{n^+-p}, it is possible that such a structure of photodetectors can be used for avalanche photodiodes [30]. It should be noted that there was no abrupt increase in photocurrent, similar to breakdown, in $PD`_{n^+-p-p^+}$ and $PD_{n^+-p-p^+}$ ($PD`_{n^+-p-p^+}$ was measured by RE without breakdown) (Fig. 8, 9).

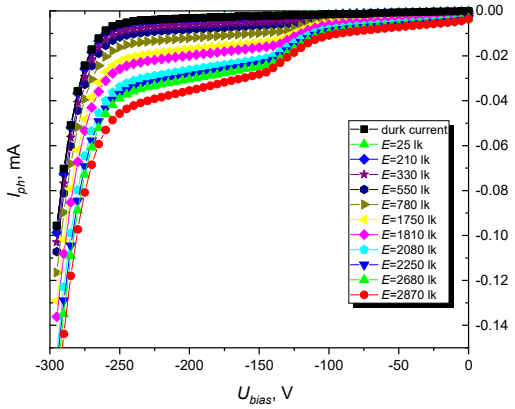

Figure 6. Light *IV*-characteristics of PD_{n^+-p} illuminated with a white light-emitting diode of different illumination

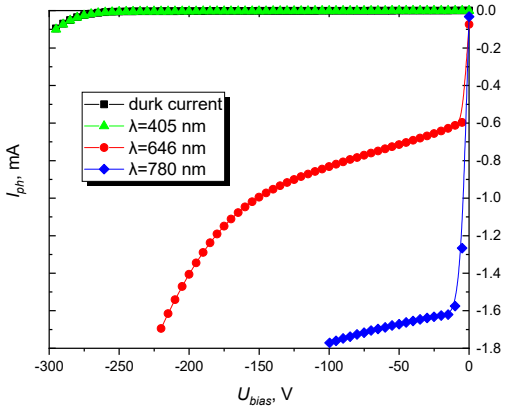

Figure 7. Light *IV*-characteristics of PD_{n^+-p} when illuminated with lasers of different wavelengths (P=5 mW)

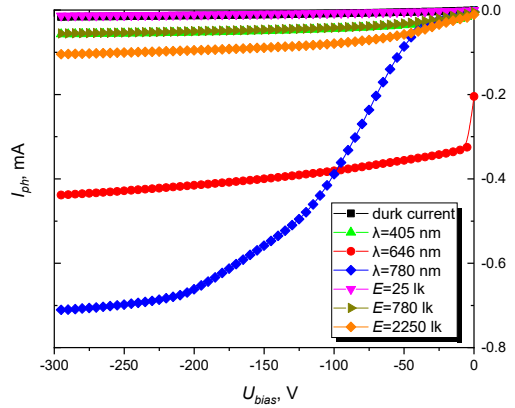

Figure 8. Light *IV*-characteristics of $PD_{n^+-p-p^+}$ illuminated with a white light-emitting diode of different illumination illuminated with lasers of different wavelengths (P=5 mW)

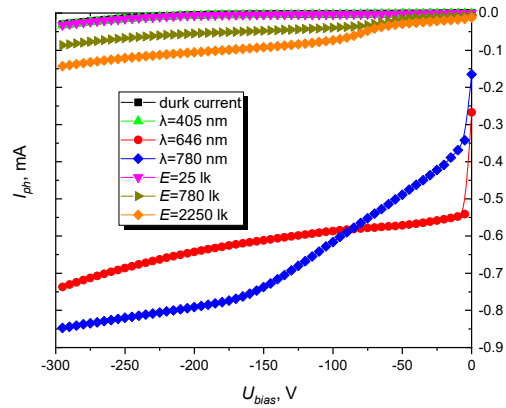

Figure 9. Light *IV*-characteristics of $PD`_{n^+-p-p^+}$ illuminated with a white light-emitting diode of different illumination illuminated with lasers of different wavelengths (P=5 mW)

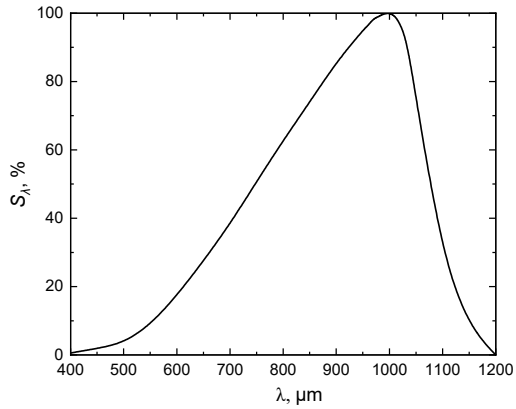

Figure 10. Typical spectral characteristics of the studied PDs

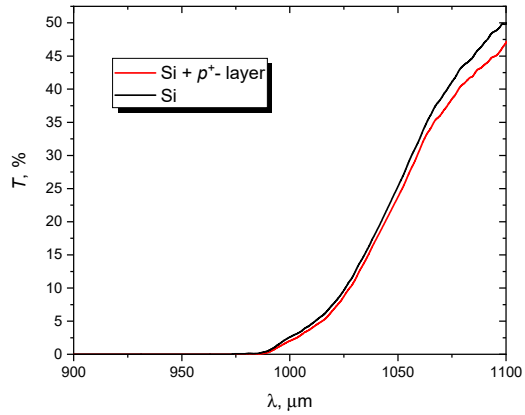

Figure 11. Transmittance spectrum of a silicon substrate and a substrate with a p^+-layer

When studying the light *IV*-characteristics with illumination with lasers of different wavelengths (Fig. 7-9), it was found that the photocurrent at λ=405 nm is virtually the same as the dark current, and with increasing wavelengths, the photocurrent increases sharply . This is due to the fact that the studied photodiodes are sensitive in the range of λ = 400-1200 nm, with a maximum of about λ = 1000 nm, respectively, at λ = 405 nm the responstivity is minimal (Fig. 10).

It should be noted that the formation of a p^+-layer in the visible wavelength range does not affect the value of the charge carrier collection coefficient and responsivity, since in this case there is no reflection of radiation from the gold mirror on the back side of the substrate due to absorption in the near-surface layers of the substrate. At λ = 1064 nm, the p^+-layer absorbs about 2% of the radiation in one pass, with increasing λ, the absorption of the p^+-layer increases (Fig. 11), but the described photodetectors are not used to detect longer wavelengths.

C) Study of the barrier capacity of structures and final electrophysical characteristics of the base material

When measuring the dependence of the capacitance (C_{RE}) of the REs on the reverse voltage, it was found that $PD_{n^+\text{-}p\text{-}p^+}$ had the lowest capacitance values, and $PD_{n^+\text{-}p}$ had the highest (Fig. 12). The difference in values is caused by the difference in the final ρ of the *i*-region (or N_A), since $C_{RE}\sim 1/\rho$ and $C_{RE}\sim N_A$ (4) [29]. Accordingly, the capacitance measurements also indicate the most effective crystal gettering in the case of $PD_{n^+\text{-}p\text{-}p^+}$, and the least effective in case of $PD_{n^+\text{-}p}$.

$$C_{RE} = A_{RE}\left(\frac{\varepsilon\varepsilon_0 eN_A}{2(\phi_c - U_{bias})}\right)^{\frac{1}{2}} \quad (4)$$

where A_{RE} is the area of REs.

If we also determine the resistivity and the diffusion length (L_n) of the minority charge carriers according to the methodology given in [31] (Table 1), we obtain:

Table 1. Values of ρ and L_n of PDs

Parameter	$PD_{n^+\text{-}p\text{-}p^+}$	$PD`_{n^+\text{-}p\text{-}p^+}$	$PD_{n^+\text{-}p}$
ρ, kΩ	14.7-15.7	11-11.6	8.5-9.5
L_n, μm	70-80	50-55	-

Note: the voltage at which the SCR reached the entire thickness of the crystal of $PD_{n^+\text{-}p}$ was chosen as the breakdown voltage of $|U_{bias}| = 230$ V.

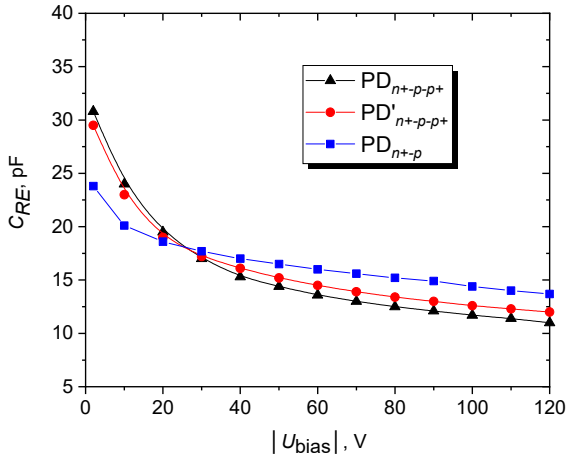

Figure 12. The dependence of the C_{RE} on the reverse voltage.

The data from Table 1 show that $PD_{n^+\text{-}p\text{-}p^+}$ have the lowest degree of degradation of the electrophysical characteristics of silicon in the process of manufacturing photodiodes, respectively, the technological route with CDP on the back side of the substrate before boron diffusion allows to obtain the most efficient PDs with the lowest values of dark currents and capacitance, as well as the highest resposivity among the studied variants of structures.

CONCLUSIONS

The photovoltaic properties of silicon n^+-p-p^+-structures and p-i-n photodiodes fabricated on their basis have been investigated. The following conclusions have been made:

1. Boron doping of the back side of the photodetector substrate significantly improves their parameters. During the boron diffusion operation, the n^+-layer also functions as a getter too.

2. Chemical dynamic polishing of the back side of the wafers before boron diffusion reduces the dark currents of photodetectors and improves the final electrophysical characteristics of silicon, in particular, the resistivity of the *i*-region and the diffusion length of minority charge carriers.

3. Photodiodes made without an p^+-layer are characterized by a breakdown of the p-n junction in the reverse voltage range of 230-260 V, which significantly increases their sensitivity and photocurrent. Presumably, such structures can be considered as possible for avalanche photodiodes.

ORCID

Mykola S. Kukurudziak, https://orcid.org/0000-0002-0059-1387; **Eduard V. Maistruk**, https://orcid.org/0000-0002-9025-6485
Ivan P. Koziarskyi, https://orcid.org/0000-0002-4984-4349

REFERENCES

[1] K. K. Samarkhanov, Applied Radiation and Isotopes, 111503 (2024). https://doi.org/10.1016/j.apradiso.2024.111503
[2] S. Khan, Instrumentation and Science Applications, 51-81 (2020). https://doi.org/10.1007/978-3-030-23201-6_5
[3] Y. Xu, & Q. Lin, Applied Physics Reviews, **7**(1) (2020). https://doi.org/10.1063/1.5144840
[4] K. Schneider-Hornstein, B. Goll, & H. Zimmermann, IEEE Photonics Journal, **15**(3), 1-9 (2023). https://doi.org/10.1109/JPHOT.2023.3279935
[5] M.S. Kukurudziak, and E.V. Maistruk, Semicond. Sci. Technol. 38, 085007 (2023). https://doi.org/10.1088/1361-6641/acdf14
[6] S. Meng-Ju, and E. G. Hemme, Semicond. Sci.Technol. 38, 033001 (2023). https://doi.org/10.1088/1361-6641/acb16b
[7] M.S. Kukurudziak, Semiconductor Physics, Quantum Electronics & Optoelectronics, **25**(4), 385 (2022). https://doi.org/10.15407/spqeo25.04.385
[8] R. Maeda et al., Appl. Phys. Express, **17**, 011006 (2024). https://doi.org/10.35848/1882-0786/ad16ae
[9] P. N. Vinod, Semicond. Sci. Technol., **20**, 966 (2005). https://doi.org/10.1088/0268-1242/20/9/014
[10] Tuck, B. Atomic diffusion in III-V semiconductors (CRC Press. 236, 2021)
[11] M.S. Kukurudziak, and E.V. Maistruk, in: 2022 IEEE 3rd KhPI Week on Advanced Technology (KhPIWeek) (IEEE, Kharkiv, 2022), pp. 1-6. https://doi.org/10.1109/KhPIWeek57572.2022.9916420
[12] M.S. Kukurudziak and E.V. Maistruk, in: Fifteenth International Conference on Correlation Optics, 121261V (SPIE, Chernivtsi, 2021). https://doi.org/10.1117/12.2616170
[13] D. Yan, et al., Solar Energy Materials and Solar Cells, **152**, 73-79 (2016). https://doi.org/10.1016/j.solmat.2016.03.033
[14] De. Salvador et al., B—Condensed Matter and Materials Physics, **81**(4), 045209 (2010). https://doi.org/10.1103/PhysRevB.81.045209
[15] S. Mirabella, et al. Journal of Applied Physics, **113**(3) (2013). https://doi.org/10.1063/1.4763353
[16] A. Y. Liu, et al. Solar Energy Materials and Solar Cells, **234**, 111447 (2022). https://doi.org/10.1016/j.solmat.2021.111447
[17] Q. Zhang, et al., RSC advances, **14**(8), 5207-5215 (2024). https://doi.org/10.1039/D3RA08772G
[18] O. E. Setälä, et al., ACS photonics, **10**(6), 1735-1741 (2023).
[19] A, Šakić, et al., Solid-state electronics, **65**, 38-44 (2011). https://doi.org/10.1016/j.sse.2011.06.042
[20] Z. Xia, et al., Applied Physics Letters, **111**(8) (2017). https://doi.org/10.1063/1.4985591
[21] M.S. Kukurudziak, Him. Fiz. Tehnol. Poverhni, **14**(1), 42 (2023). https://doi.org/10.15407/hftp14.01.042 (in Ukrainian)
[22] K.V. Ravi, Imperfections and impurities in semiconductor silicon, (Wiley, New York, 1981).
[23] J. Bauer, et al., Progress in Photovoltaics: Research and Applications, **21**(7), 1444-1453 (2013). https://doi.org/10.1002/pip.2220
[24] N. Rouger, COMPEL: The International Journal for Computation and Mathematics in Electrical and Electronic Engineering, **35**(1), 137-156 (2016). https://doi.org/10.1108/COMPEL-12-2014-0330
[25] O. Breitenstein, IEEE Transactions on Electron Devices, **57**(9), 2227-2234 (2010). https://doi.org/10.1109/TED.2010.2053866
[26] B. J. Baliga, Fundamentals of Power Semiconductor Devices, 89-170 (2019). https://doi.org/10.1007/978-3-319-93988-9_3
[27] M.S. Kukurudziak, East Eur. J. Phys. **2**, 289 (2023), https://doi.org/10.26565/2312-4334-2023-2-33
[28] A.V. Fedorenko, Technology and design in electronic equipment, **17**(3–4), 17 (2020). https://doi.org/10.15222/ TKEA2020.3-4.17 (in Ukrainian)
[29] N.M. Tugov, B.A. Glebov, and N.A. Charykov, Semiconductor devices: Textbook for universities, edited by V.A. Labuntsov, (Energoatomizdat, Moscow, 1990). (in Russian)
[30] J. C. Campbell, Journal of Lightwave Technology, **34**(2), 278-285 (2015). https://doi.org/10.1109/JLT.2015.2453092
[31] M.S. Kukurudziak, East Eur. J. Phys. **2**, 345 (2024). https://doi.org/10.26565/2312-4334-2024-0-41

ВПЛИВ ДИФУЗІЇ БОРУ НА ФОТОЕЛЕКТРИЧНІ ПАРАМЕТРИ n^+-p-p^+-КРЕМНІЄВИХ СТРУКТУР ТА ФОТОПРИЙМАЧІВ НА ЇХ ОСНОВІ

Микола С. Кукурудзяк[a,b], Едуард В. Майструк[b], Іван П. Козярський[b]
[a]АТ «Центральне конструкторське бюро Ритм», 58032, м. Чернівці, вул. Головна, 244, Україна
[b]Чернівецький національний університет імені Юрія Федьковича, 58002, м. Чернівці, вул. Коцюбинського, 2, Україна

У статті досліджено фотоелектричні властивості кремнієвих n^+-p-p^+-структур та фотодіодів виготовлених на їх основі. Встановлено, що проведення дифузії бору в зворотну сторону підкладки крім створення омічного контакту гетерує генераційно-рекомбінаційні центри, що дозволяє знизити темновий струм фотодіодів та підвищити їх чутливість. Також встановлено, що хіміко-динамічне полірування зворотної сторони підкладок власне перед дифузією бору дозволяє ліквідувати значну кількість дефектів та покращити кінцеві параметри виробів. В зразків без p^+-шару та зразків не полірованих зі зворотної сторони спостерігається пробій p-n переходу, що спричинено розширенням області просторого заряду на всю товщу підкладки та його досягненням дефектної зворотної сторони кристалу.

Ключові слова: *кремній; фотоприймачі; лавинні фотодіоди; темновий струм; ізовалентна домішка; чутливість*